Journal of Computational Interdisciplinary Sciences (2011) 2(2): 93-98

Printed version ISSN 1983-8409 / Online version ISSN 2177-8833
http://epacis.net
doi: 10.6062/jcis.2011.02.02.0036

Investigating the influence of inversion methods in extrapolated magnetic fields of the solar corona

Tereza S.N. Pinto and Joaquim E.R. Costa

Manuscript received on September 23, 2010 / accepted on August 15, 2011

ABSTRACT

The solar magnetic field at coronal level is responsible for phenomena such as solar flares and coronal mass ejections. It is thus of interest to investigate the topological features that create the conditions for these events to occur. At the corona, the magnetic field is considered to be a force free field: $\nabla \times \vec{B} = \alpha \vec{B}$. If α is a constant the force free field is linear and the differential equation has known solutions, such as the Fourier transform solution [1]. The boundary conditions are given by magnetograms, maps of the magnetic field at photospheric level. The magnetograms are produced from measurements of the Stokes parameters in spectral lines and application of inversion methods to derive the three components of the magnetic field. Apart from intrinsic issues (e.g. Zeeman saturation effect), the production of these maps must deal with other issues, such as noise and the instrument spectral and spatial resolution, and assumptions in the inversion method. We investigate what are the consequences for the extrapolated magnetic field due to boundary conditions determined from different sets of magnetograms. We aim to estimate the inaccuracies induced by the inversion codes in our method of extrapolation, comparing extrapolations from sets of data of two instruments: the Michelson Doppler Imager (MDI) on board SOHO observatory and the Spectro-Polarimeter (SP) of the Solar Optical Telescope (SOT) on board Hinode spacecraft. Thus, we evaluate the correlations and compare the topological features of the MDI and SP-SOT extrapolations.

Keywords: computational physics, solar physics, force free fields, inversion methods.

1 INTRODUCTION

The magnetic field plays an important role in several phenomena at solar corona: active regions, solar flares, coronal heating and others. As usual in astrophysics, methods have been developed to observe this field and compare it to theoretical models. The observation of magnetic fields is indirect and only possible due the Zeeman effect in spectral lines.

The Zeeman effect is a quantum effect manifested as the splitting of a spectral line in multiplets in the presence of a magnetic field. A given atom has degeneracies characterized by the quantum numbers. Each quantum state assumes a different energy level when the magnetic dipole interacts with the field. In other words, the orbital angular momentum precesses around the direction of the magnetic field. The resulting observable is the presence of two or more shifted spectral lines equally apart from the central line. The number of lines depends on the selection rules, and the shifting ($\Delta\lambda_B$) is proportional to the magnetic field intensity (B):

$$\Delta\lambda = 6,67 \times 10^{-5} g^* \lambda^2 B \quad \text{(cgs units)} \qquad (1)$$

The shifted components ($\lambda_0 \pm \Delta\lambda$) are parallel to the line of sight and circularly polarized (each in one orientation of the

Correspondence to: Tereza S.N. Pinto
Divisão de Astrofísica, Instituto Nacional de Pesquisas Espaciais, São José dos Campos, SP, Brazil – E-mail: tereza.satiko@das.inpe.br

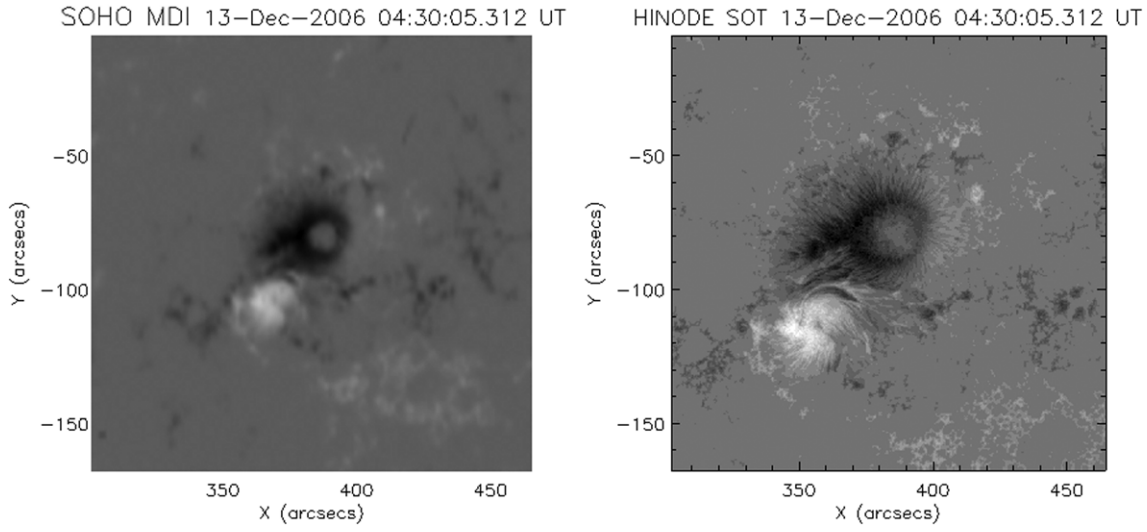

Figure 1 – MDI and SP-SOT magnetograms of active region NOAA 10930; black/white represents south/north polarity. The most noticeable feature is the SP superior spatial resolution.

field). The unshifted component is linearly polarized in a direction perpendicular to the line of sight. In the Sun only the triplet is frequently resolved. Observations of the shifted components are performed over the Sun's surface, producing maps of the magnetic intensity and orientation, the so called longitudinal magnetograms. Figure 1 shows two longitudinal magnetograms produced by instruments on board satellite observatories: the Michelson Doppler Imager (MDI) [2] on board SOHO spacecraft and the Spectro Polarimeter (SP) of the Solar Optical Telescope (SOT) [3] on board Hinode spacecraft. These two instruments produce magnetograms using different methods and instrumentation.

The MDI is a Michelson interferometer working at Ni I (6768 Å) in a 94 mÅ bandpass. It measures the Doppler shift in each circular polarization state of this absorption line. The magnetic intensities are derived by differentiation of the two polarized modes with the aplication of calibration maps. A full disk map achieving a spacial resolution of 1.98″ per CCD pixel is produced every 96 minutes. SP-SOT is a spectropolarimeter; it measures Stokes IQUV in line profiles. Then, inversion methods are applied to produce maps of the three componentes of the magnetic field. This is done in two iron lines, 6301.5 Å and 6302.5 Å in a 21.5 mÅ band pass. The magnetograms produced by this instrument achieve a superior spatial resolution, 0.31″ per CCD pixel. This means that more magnetic structures are resolved, i.e., more information is available. SP-SOT is able to produce a map (field of view of 164″) in 30 minutes.

MDI magnetograms have been a standard even though some recalibrations were performed. The last one, in 2008, improved the sensitivity map reducing the field intensities according to the position [6]. The inversion method addopted for SP is known as MERLIN [4]. It performs a least-squares fitting of the observed Stokes profiles using the Levenberg-Marquardt algorithm, taking into account a Milne-Eddington atmospheric model. In both data products some effects may appear: the 180° ambiguity and the Zeeman saturation effect. The latter can be seen in the center of the south polarity spot in Figure 1. This effect is an anticorrelation between the magnetic field intensity and the circular polarization when the intensity is above a threshold. The 180° ambiguity is the observational impossibility to define the sense of the transverse magnetic component.

Although these two instruments provides to the solar physics community important data sources, their different calibrations and inversion methods may induce different results in analysis of the same active region. In this sense, any inference over these observations must be considered with caution. Our developments in computations of magnetic fields over the solar corona may produce different outputs when the magnetograms supply even slightly different inputs. The objective of this work is to investigate if and what differences these two datasets induce in our methodology. In the next section we present our methodology for studying the magnetic field at solar corona, and the physics embebed in it. In section 3 we present our results and conclusions.

2 FORCE FREE MAGNETIC FIELDS

Both quiet atmosphere and transient events studies of the Sun requires knownledge of the magnetic phenomenology at coronal level. The observational aspects described in the previous section concern only the photospheric manifestations of the magnetic field. The field arises from the Sun's convective layer and propagates to the corona. At the corona, the plasma density and kinetic pressure decrease rapidly and the temperature is high enough (10^6K) to create an ideal conductor condition. Another condition is that the magnetic pressure is dominant in the medium. At these conditions the magnetic field is considered to be a **force free field** as the plasma is not subjected to any force. Another interpretation is that the Lorentz force is null (the spatial dependence is supressed as the equations may be generally written in any set of coordinates):

$$\vec{J} \times \vec{B} = 0 \tag{2}$$

Follows that the magnetic field is described by the following equations (derived from equation 2 and from Maxwell's equations, see [7]):

$$\nabla \times \vec{B} = \alpha \vec{B} \tag{3}$$

$$\begin{aligned} \vec{B} \cdot \nabla \alpha &= 0 \\ \nabla \cdot \vec{B} &= 0 \end{aligned} \tag{4}$$

where α is also a function of the position and represents the distribution of current density. Equation 3 is the fundamental equation describing a force free field and it shows that the current density (α) is parallel to the magnetic field in any point of space. Equations 4 give other properties of this field: α is a constant along a field line and the field satisfies the solenoidal condition.

From equation 3 we see that modelling a force free for the solar corona is not an easy task, as it is a non linear differential equation. A first approximation is to consider the linearization of the system. In this case, equation 3 turns into a Helmholtz equation and analytical solutions are known. Nakagawa and Raadu (1972) [1] proposed a solution by Fourier transforms giving the magnetic field components explicitly by:

$$\begin{aligned} B_x &= \textstyle\sum_{k\neq 0} \frac{i}{k^2}\left[\alpha k_y - k_x(k^2-\alpha^2)^{1/2}\right] \\ &\quad \times \vec{B}_k \ \exp\left[i\vec{k}\cdot x - (k^2-\alpha^2)^{z/2}\right] \\ B_y &= \textstyle\sum_{k\neq 0} \frac{-i}{k^2}\left[\alpha k_x + k_y(k^2-\alpha^2)^{1/2}\right] \\ &\quad \times \vec{B}_k \ \exp\left[i\vec{k}\cdot x - (k^2-\alpha^2)^{z/2}\right] \\ B_z &= \textstyle\sum_{k\neq 0} \vec{B}_k \ \exp\left[i\vec{k}\cdot x - (k^2-\alpha^2)^{z/2}\right] \end{aligned} \tag{5}$$

where $\vec{B}_k$ is related to the observed field B_z at the photosphere:

$$B_z(x, y, z = 0) = B_{00} + \sum_{k\neq 0} B_k \ \exp(i\vec{k}\cdot\vec{x}) \tag{6}$$

B_{00} is the average intensity of the observed field at $z = 0$. $\vec{k}$ is unitary and can be decomposed as

$$\vec{k} = k_x\hat{x} + k_y\hat{y} \tag{7}$$

This method does not provide an unique solution, as it is an ill posed problem. On the other hand, it has only α as a free parameter that indicates the sense and the intensity of the stress applied to the field lines. The solutions for B_x, B_y and B_z were implemented in IDL 7.0 considering the advantages of the Fast Fourier Transform algorithm when computing the B_k's. As the solution method requires, each magnetic field component is calculated in a finite space defined as a section of the magnetogram. The attained height at the corona was defined as 100 pixels of the MDI magnetogram and the field so obtained is said to be an extrapolated magnetic field.

The active region NOAA 10930 was observed by SP-SOT in 2006-12-13 at 04:30 UT and by MDI at 04:51 UT of the same date. MDI data was differentially rotated to correct the time difference. SP-SOT data was rescaled to the same grid size as MDI and the most correlated areas (correlation coefficient of 0.87) containig the active region were extracted.

3 RESULTS AND DISCUSSION

Figure 2 shows a force free extrapolations for the cases $\alpha = 0$, or the potential field extrapolation and for $\alpha \neq 0$, or the linear field extrapolation. This potential field is the lower energy configuration, and increasing the energy content means introducing stress, or torsion on the magnetic field lines. The topologycal differences are evident and represent one of the physical aspects we deal with when studying the coronal magnetic field: which configuration reproduces with fidelity the real situation? This is an open problem, as there are no realiable solutions to the non linear force free equation, nor observations of the magnetic field at coronal level. At the moment we limit ourselves to the discussion of the influences of the methods to produce the magnetograms on the extrapolations codes. Thus, we compare potential and linear extrapolations over MDI and SP-SOT data at different heights: photosphere, low and high corona.

Figure 3 shows comparisons of the extrapolated magnetic fields. In general, the field lines attained typical heights of 4.851

$\times$ 10^9 cm and 5.544 $\times$ 10^9 cm for SOT/SP and MDI respectively (potential case). In other words, MDI extrapolations had magnetic loops at higher altitudes. In the linear case, we obtained maximum heights superior to 1.39 $\times$ 10^{10} cm for both data sets. SOT/SP extrapolations obtained a greater number of magnetic field lines, 100 against 83.

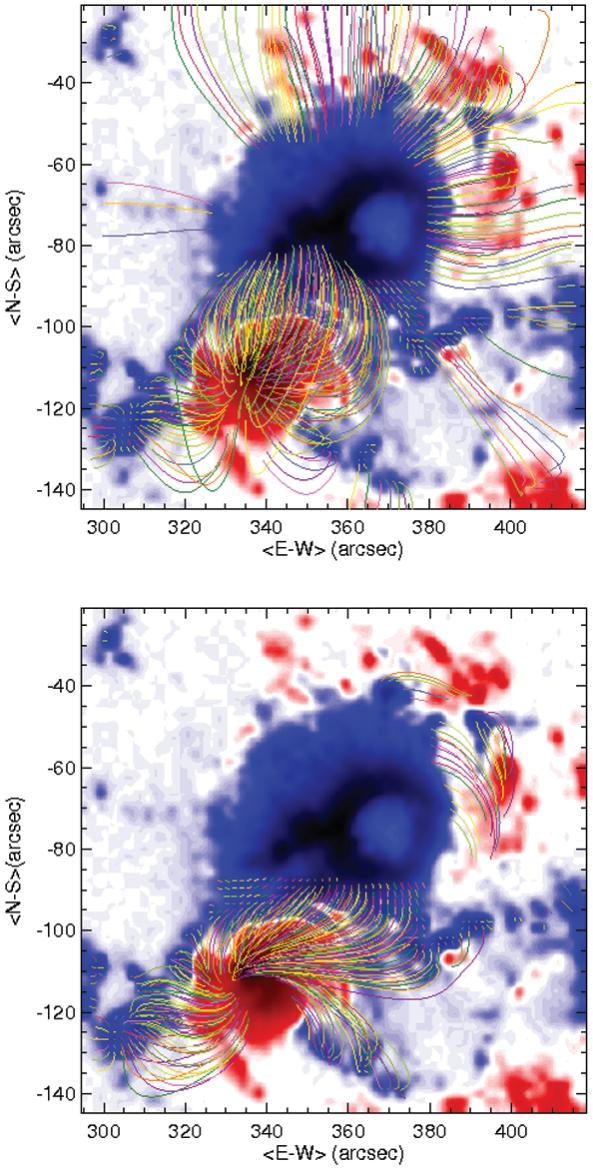

Figure 2 – Potential (top) and linear (bottom) field extrapolations over MDI data of active region NOAA 10930. The south polarity is in blue, the north polarity is in red and white represents the average intensity.

At photospheric level it is expected that the extrapolation reproduces the observations, and we verified that the correlation coefficient for SOT/SP was of 0.90 while for MDI was of 0.71 (potential case, with similar results for the linear case). The mean magnetic intensities were greater for MDI extrapolations in both cases (potential and linear). This result contradicts those obtained by Wang et al. (2009) [8], but they compared only the data sets and excluded the saturated region. However, as the two magnetograms and the two extrapolations at photospheric level correlated similarly, we did not excluded this region as this procedure would modify the extrapolation results. At the corona the magnetic intensities were also greater for MDI extrapolations, both in potential and linear cases.

To conclude, in this case of study we verified that the magnetograms generated by an inversion code and a calibration method yield to slightly different extrapolations. The influence of the inversion code was clear only in the maximum height of the magnetic field lines obtained in the potential condition. Other results are more likely to be due the spatial resolution of the data, since they arise at the photosphere. This has implications when one wants to deduce a physical property of the flaring region based on extrapolated magnetic fields. For example, the energy content of the MDI extrapolation in the potential case was E_{MDI} = 3.5 $\times$ 10^{13} erg, and for the SOT/SP was of E_{SOT} = 1.9 $\times$ 10^{13} erg (E_{MDI}/E_{SOT} = 1.84). Our purpose in using magnetic extrapolations is to obtain brightness maps of flaring loops considering the radiative transfer through the magnetic enviroment. In this sense, SOT-SP data has the advantage of providing the three componentes of the magnetic field, which will lead to more precise extrapolations. The direct comparison of the extrapolations with the flaring loops as seen in extreme ultraviolet observations is another way to evaluate the extrapolations, and tools to do such a comparison are under development [9].

ACKNOWLEDGMENTS

We thank MDI/SOHO and SP-SOT/Hinode for the data.

REFERENCES

[1] NAKAGAWA Y & RAADU MA. 1972. On pratical representation of magnetic field. Solar Physics, v. 1, 25: 127–135.

[2] SCHERRER PH et al. 1995. The solar oscillations investigation – Michelson Doppler Imager. Solar Physics, v. 1, 162: 129–188.

[3] TSUNETA S et al. 1995. The Solar Optical Telescope for the Hinode Mission: An Overview. Solar Physics, v. 2, 249: 167–196.

[4] http://www.csac.hao.ucar.edu/csac/nextGeneration.jsp, last access: 2010-08-19.

[5] BENTLEY RD & FREELAND SL. 1998. SOLARSOFT: an analysis environment for solar physics, Crossroads for European Solar and

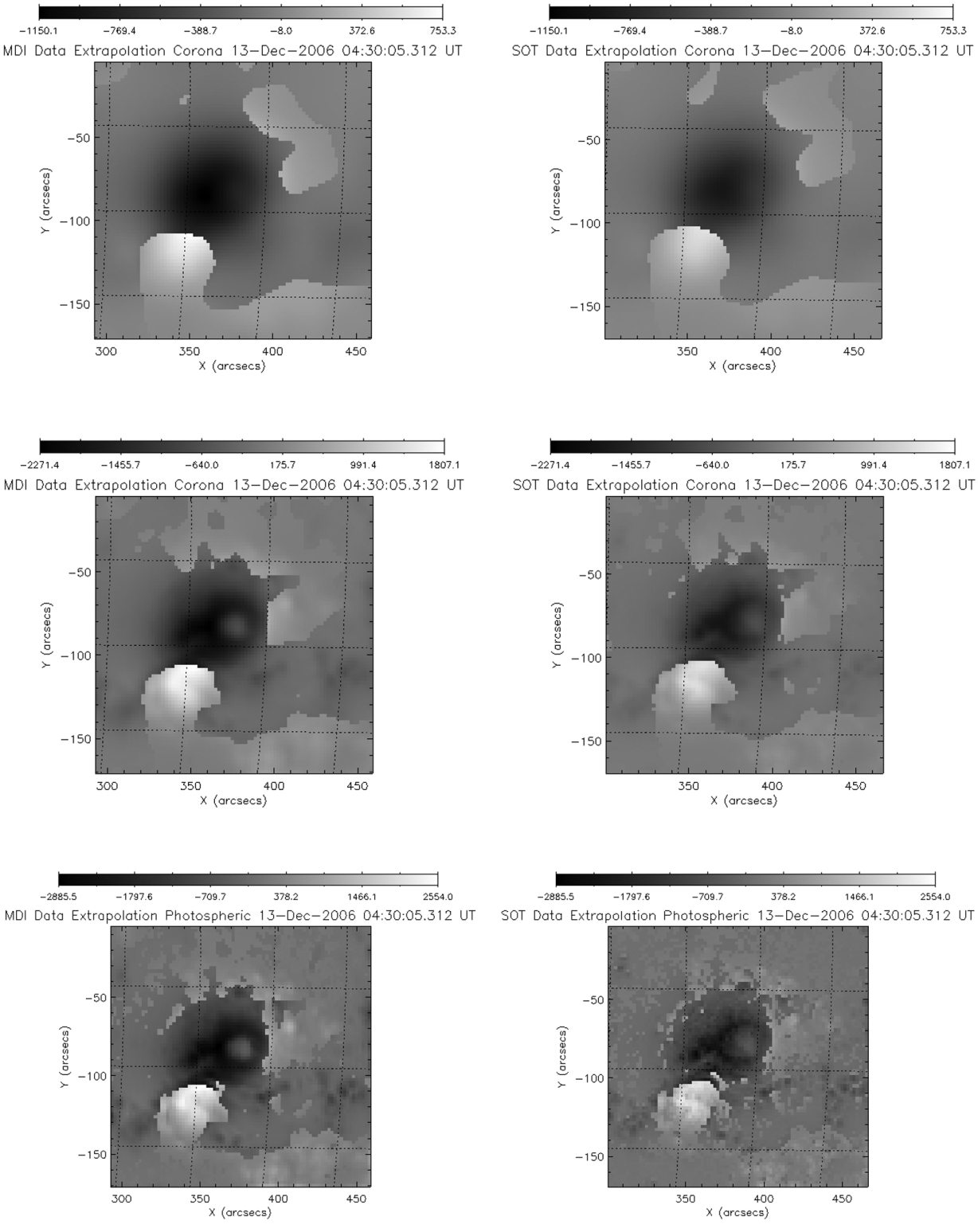

Figure 3 – MDI (left) and SOT/SP (right) linear force free extrapolations of the magnetic field over NOAA 10930 at the high corona (top), low corona (middle) and photosphere (bottom images).

Heliospheric Physics. Recent Achievements and Future Mission Possibilities. ESA Special Publication, 417: 225–228.

[6] http://soi.stanford.edu/magnetic/Lev1.8/, last access: 2010-09-19.

[7] SAKURAI T. 1989. Computational modeling of magnetic fields in solar active regions. Space Science Reviews, 51: 11–48.

[8] WANG D, ZHANG M, LI H & ZHANG HQ. 2009. A cross-comparison of cotemporal magnetograms obtained with MDI/SOHO and SP/Hinode. Solar Physics, v. 1, 260: 233–244.

[9] SILVA CW, COSTA JER & ROSA RR. 2010. A computational approach for the recognition of the magnetic field lines on Solar Corona, 1st Conference on Computational Interdisciplinary Sciences, São José dos Campos.